

upon chilling these duplexes collapse into single-stranded DNA, which is susceptible to nuclease digestion. In contrast, while heating also separates the strands of the replicative forms, their covalent linkage through terminal hairpins leads to rapid reannealing after chilling; the resulting double-stranded DNA molecules are resistant to nuclease digestion (nicking of the replication forms would prevent snap-back, leading to the apparent difference in quantity of hairpin forms in Fig. 3 compared to Fig. 2B).

Inhibition of erythroid but not myeloid colony formation has been observed after infection of normal human bone marrow cells with B19 (11). A similar specificity of B19 for erythroid cell progenitors was demonstrated in suspension cultures (Table 1). Production of B19 was proportional to the erythroid content of the bone marrow cell samples. Replication of B19 was greatly enhanced by the addition of erythropoietin but only slightly increased by the use of conditioned media containing colony-stimulating factors and burst-promoting activity. These results indicate that the target cell of the B19 in suspension cultures is a precursor to mature erythrocytes, probably more responsive to erythropoietin than to factors operating on less mature hematopoietic progenitors.

A large number of cell lines have been tested unsuccessfully for their ability to propagate B19 virus. Dot blot analysis of DNA from B19-inoculated K562 (14) and HEL (15) erythroleukemia cell lines, even after hemin induction, failed to show the presence of B19 DNA within whole cells or nuclei (Fig. 1), despite the erythroid features of these cell types. However, virus obtained from human erythroid bone marrow cultures contained the characteristic B19 proteins as detected by immunofluorescence and immunoblotting, and the supernatants of these cultures were more infectious than serum containing virus (10). Bone marrow culture may represent the only feasible current method for the propagation and study of B19 parvovirus in vitro, and it may be safer than attempting to adapt parvoviruses to tissue culture (9). The target and site of replication of the B19 virus appear to be an immature cell in the erythroid lineage. Molecular analysis of suspension cultures should allow determination of the basis for the specificity of the B19 parvovirus for erythroid cells, evident from both culture and clinical observations. The tissue tropism of this virus may be utilizable in the construction of vectors specific to erythroid progenitors for the treatment of human hemoglobinopathies by stem-cell transfection.

#### REFERENCES AND NOTES

1. Y. E. Cossart, A. M. Field, B. Cant, D. Widdows, *Lancet* **1975-I**, 71 (1975).
2. J. R. Pattison *et al.*, *ibid.* **1981-I**, 664 (1981); G. R. Serjeant *et al.*, *ibid.* **1981-II**, 595 (1981).
3. M. J. Anderson *et al.*, *ibid.* **1983-I**, 1378 (1983).
4. D. G. White *et al.*, *ibid.* **1985-I**, 419 (1985); D. M. Reid, T. M. S. Reid, T. Brown, J. A. N. Rennie, C. J. Eastmond, *ibid.*, p. 422.
5. P. D. Knott, G. A. C. Welby, M. J. Anderson, *Br. Med. J.* **289**, 1660 (1984); T. Brown, A. Anand, L. D. Ritchie, J. P. Clewley, T. M. S. Reid, *Lancet* **1984-II**, 1033 (1984).
6. J. Summers, S. E. Jones, M. J. Anderson, *J. Gen. Virol.* **64**, 2527 (1983).
7. J. Clewley, *ibid.* **65**, 241 (1984).
8. S. Cotmore and P. Tattersall, *Science* **226**, 1161 (1984).
9. G. Siegl, in *The Parvoviruses*, K. I. Berns, Ed. (Plenum, New York, 1984), pp. 363-388.
10. K. Ozawa *et al.*, unpublished data.
11. P. P. Mortimer, R. K. Humphries, J. G. Moore, R. H. Purcell, N. S. Young, *Nature (London)* **302**, 426 (1983).
12. U. M. Saarinen *et al.*, *Blood* **67**, 1411 (1986).
13. New synthesis of B19 parvovirus in vitro was inferred from two other experiments (K. Ozawa, G. Kurtzman, N. Young, in preparation). Viral output into supernatant varied with the multiplicity of infection (MOI), and at low MOI 50× the input virus was present in culture fluids. In addition, [<sup>35</sup>S]methionine-labeled capsid proteins were present in the particulate fraction after sucrose gradient sedimentation of culture supernatants.
14. C. B. Lozzio and B. B. Lozzio, *Blood* **45**, 321 (1980).
15. P. Martin and T. Papayannopoulou, *Science* **216**, 1233 (1982).
16. N. N. Iscove and F. Melchers, *J. Exp. Med.* **147**, 923 (1979).
17. Gift from P. Tattersall.
18. K. Ozawa *et al.*, *Biochem. Biophys. Res. Commun.* **130**, 257 (1985).
19. W. W. Hauswirth, in *The Parvoviruses*, K. I. Berns, Ed. (Plenum, New York, 1984), pp. 129-152.
20. We thank P. Tattersall for the generous gift of pYT103 and for helpful advice in the interpretation of these studies and M. Harrison for preparing the electron micrograph.

13 January 1986; accepted 28 May 1986

## Calcium Rises Abruptly and Briefly Throughout the Cell at the Onset of Anaphase

MARTIN POENIE, JANET ALDERTON, RICHARD STEINHARDT, ROGER TSJEN

**Continuous measurement and imaging of the intracellular free calcium ion concentration ( $[Ca^{2+}]_i$ ) of mitotic and interphase PtK<sub>1</sub> cells was accomplished with the new fluorescent  $Ca^{2+}$  indicator fura-2. No statistically significant difference between basal  $[Ca^{2+}]_i$  of interphase and mitotic cells was detected. However, mitotic cells showed a rapid elevation of  $[Ca^{2+}]_i$  from basal levels of 130 nM to 500 to 800 nM at the metaphase-anaphase transition. The  $[Ca^{2+}]_i$  transient was brief, lasting approximately 20 seconds and the elevated  $[Ca^{2+}]_i$  appeared uniformly distributed over the entire spindle and central region of the cell. The close temporal association of the  $[Ca^{2+}]_i$  transient with the onset of anaphase suggests that calcium may have a signaling role in this event.**

**T**HE ONSET OF ANAPHASE IS AN abrupt transition characterized by the separation of chromatids at the metaphase plate followed by the rapid displacement of chromosomes toward the poles. The localization of calcium-sequestering activity and calmodulin in the spindle region (1, 2), the alteration of metaphase transit times by manipulation of intracellular or extracellular calcium (3, 4), the sensitivity of microtubule polymerization to calcium (5), and the mitotic arrest caused by a variety of calmodulin inhibitors (6, 7), all point to a possible regulatory role for cytoplasmic calcium ions in mitosis. We previously reported measurements of intracellular free calcium ion concentration ( $[Ca^{2+}]_i$ ) during the first cell division cycle of fertilized *Lytechinus pictus* eggs; we detected a brief calcium transient in close temporal proximity to the metaphase transition (8). However, since we could not resolve the chromosomes in these eggs, the exact timing

of the metaphase-anaphase transition in relation to the calcium transient could not be determined. We also did not determine the spatial distribution of  $[Ca^{2+}]_i$  during these measurements. Keith *et al.* (9) measured  $[Ca^{2+}]_i$  in PtK<sub>2</sub> cells with quin-2 and did not detect a calcium transient, but reported that average  $[Ca^{2+}]_i$  declined during mitosis (9). In another study Keith *et al.* found that calcium did rise at the poles during the metaphase-anaphase transition in *Haemaphysalis* cells (10).

Here we report the measurement of  $[Ca^{2+}]_i$  during mitosis in PtK<sub>1</sub> cells with fura-2, a new fluorescent indicator of  $[Ca^{2+}]_i$  (11, 12). Fura-2 signals increased  $[Ca^{2+}]_i$  by an increase in the ratio of 350-nm to 385-nm excitation efficiency, which was quantified by either a photomultiplier

M. Poenie and R. Tsien, Department of Physiology-Anatomy, University of California, Berkeley, CA 94720. J. Alderton and R. Steinhardt, Department of Zoology, University of California, Berkeley, CA 94720.

or a video silicon-intensified target camera and digital image processing. The favorable cytology of PtK<sub>1</sub> cells combined with both whole-cell photometry and imaging has made it possible to determine the duration, magnitude, and spatial distribution of calcium transients during the metaphase-anaphase transition of these cells. We have found that a brief calcium transient occurs within seconds of the metaphase-anaphase transition, which lasts about 20 seconds, and rises to approximately 500 to 800 nM. Furthermore, there is no obvious [Ca<sup>2+</sup>]<sub>i</sub> gradient during the transient. However, we have consistently seen that [Ca<sup>2+</sup>]<sub>i</sub> within the spindle region is lower than in the surrounding cytoplasm prior to the metaphase transition.

Figure 1 shows the calcium transient at the time of the metaphase-anaphase transition recorded from a single PtK<sub>1</sub> cell with a photomultiplier. At the start of the measurement, the chromatids were still attached at their kinetochores. During the recording period, a large calcium transient was detected that lasted about 20 seconds as [Ca<sup>2+</sup>]<sub>i</sub> rose to 800 nM (13). Immediately after the Ca<sup>2+</sup> transient, observation of the cell revealed that chromosomes had separated and poleward chromosome movement had started. These transients were observed in all five experiments in which cells progressed into anaphase. Cells that did not show the [Ca<sup>2+</sup>]<sub>i</sub> rise also did not progress to anaphase or else the trapped fura-2 had leaked out so that they were no longer responsive to ionophore.

An example of [Ca<sup>2+</sup>]<sub>i</sub> imaging can be seen in Fig. 2. This sequence begins (*t* = 0) with a transmitted-light picture of a metaphase cell, typical of the starting point for the photometer measurements shown in Fig. 1. A computer-processed image of the 350 nm/385 nm excitation ratio of fura-2 fluorescence from the same cell was produced 17 seconds after the transmitted-light picture. This pseudocolor display assigned hues to represent a 12-fold range of ratios on a logarithmic scale. Increasing fura-2 350 nm/385 nm ratios and [Ca<sup>2+</sup>]<sub>i</sub> corresponded to hues ranging from blue to green, yellow, red, and purple (14). The color scale in Fig. 2 gives an approximate calibration for [Ca<sup>2+</sup>]<sub>i</sub> in μM. In the cell shown at *t* = 17 seconds, [Ca<sup>2+</sup>]<sub>i</sub> was generally low. Areas outside the spindle showed calcium concentrations of approximately 180 to 220 nM and appeared as green-yellow in the pseudocolor display. In the spindle region, however, [Ca<sup>2+</sup>]<sub>i</sub> was slightly lower, 110 to 150 nM, and appeared blue in the pseudocolor display. At *t* = 9 minutes 39 seconds, visual inspection revealed that the chromatids were still tied together and morphologically the

cell was unchanged from the starting point. However, there was a slight increase in [Ca<sup>2+</sup>]<sub>i</sub> as revealed by the loss of blue in the spindle region of the cell.

The first significant rise in [Ca<sup>2+</sup>]<sub>i</sub> was seen at *t* = 11 minutes 18 seconds (Fig. 2); the shift of the pseudocolor to red indicates [Ca<sup>2+</sup>]<sub>i</sub> of 480 to 540 nM over most of the central region of the cell. The brevity of this transient is revealed by the image taken 15 seconds later in which [Ca<sup>2+</sup>]<sub>i</sub> had already returned to basal levels. The spindle poles remained slightly elevated although their conspicuous appearance is mainly due to a higher brightness level in the pseudocolor display (14). A subsequent transmitted-light image, taken at *t* = 11 minutes 57 seconds, shows that the onset of anaphase had occurred. These pictures reveal that a calcium transient occurs near the time of the metaphase-anaphase transition, although precise overlap cannot be proved since the fluorescence and transmitted-light images could not be taken simultaneously. These results are a direct demonstration of an elevation of [Ca<sup>2+</sup>]<sub>i</sub> during the metaphase-anaphase transition in cultured animal cells. Other [Ca<sup>2+</sup>]<sub>i</sub> fluctuations during mitosis were negligible by comparison; whole-cell [Ca<sup>2+</sup>]<sub>i</sub> for 20 mitotic cells was 132 ± 29 nM (mean ± SD) excluding the transient, whereas 78 interphase cells averaged 129 ± 29 nM.

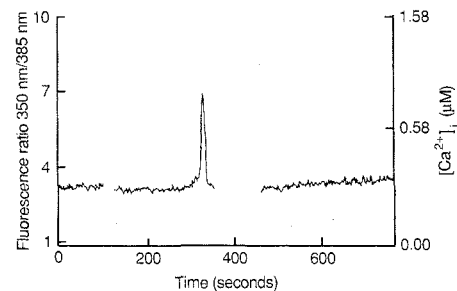
Though fura-2 is much more suitable than quin-2 for fluorescence ratio measurements, two problems with fura-2 can hinder

the accurate calibration of [Ca<sup>2+</sup>]<sub>i</sub>. (i) Increased viscosity somewhat decreases the 350 nm/385 nm ratio, an effect for which we have attempted to compensate in the calibration of Figs. 1 and 2 (13). The effect of the viscosity correction is mainly at low [Ca<sup>2+</sup>]<sub>i</sub> and is much too small for a transient loss in viscosity to have simulated the observed [Ca<sup>2+</sup>]<sub>i</sub> rise. (ii) Fura-2 can gradually become sequestered into organellar compartments (15, 16), a process whose rapidity depends strongly on temperature and cell type. In these experiments, sequestration was minimized by loading the cells at room temperature, then immediately observing them at 37°, or at 32°C (a temperature that retards dye compartmentalization more than it slows mitosis). Most measurements were made at 32°C; the 0.5 hour in which cells contain useful intracellular dye concentrations is further reduced at 37°C.

Cells were studied only if their fluorescence was generally diffuse as in Fig. 2, consistent with dye being mainly in the cytosol. However, the localized brightness at the spindle poles in Fig. 2 may suggest that some dye had accumulated or been sequestered here. This dye was not exposed to as high a transient [Ca<sup>2+</sup>]<sub>i</sub> as the rest of the cell at 11 minutes 18 seconds, so dye sequestration would seem, if anything, to cause underestimation of the amplitude and wide distribution of the pulse.

Another cause of punctate fluorescence can sometimes be the endocytosis of parti-

Fig. 1. Calcium transient at the metaphase-anaphase transition in a single PtK<sub>1</sub> cell. PtK<sub>1</sub> cells were more difficult to load with fura-2 than most other mammalian cell types we have tried. Loading was further complicated by the apparent ability of these cells to gradually compartmentalize and extrude intracellular fura-2, a process that was particularly rapid at 37°C. To attain uniform loading at sufficiently high intracellular concentration for photometry and imaging a modified loading regime was necessary. Cells were placed in a modified Ham's F-12 medium lacking bicarbonate, phenol red, and riboflavin, but containing 10 mM Hepes buffer and 2% fetal calf serum. To load cells in a dish containing 3 ml of medium, 5 μl of 10 mM fura-2 acetoxyethyl ester (Molecular Probes, Junction City, OR) in dimethyl sulfoxide (DMSO) was premixed first with 2.5 μl of 25% w/w Pluronic F-127 (BASF Wyandotte Corp., Wyandotte, MI) in DMSO. Pluronic F-127 is a nonionic dispersing agent that helps solubilize large dye molecules in physiological media (17). Subsequently, 75 μl of calf serum was added to the dye mixture and, after mixing, the final solution was transferred to the petri dish with gentle agitation of the dish. Cells were incubated at room temperature for 1 to 2 hours on an orbital shaker oscillating at 40 rev/min. After the incubation, the loading solution was replaced with fresh medium and the incubation continued at 32°C (usually on the microscope stage). We did not observe any effect of fura-2 on rate or frequency of mitosis. PtK<sub>1</sub> cells were plated onto 15-mm plastic petri dishes modified so that glass coverslips replaced part of the bottom of the dish. Platings were carried out 1 to 2 days before the cells were used. Single-cell measurements with the photometer were carried out essentially as described (8). Cells were measured continuously from metaphase through anaphase or sometimes through cleavage, except for periodic brief interruptions to determine the progress through mitosis. The measurement shown here begins with the cell in metaphase similar to that shown in Fig. 2. Fluorescence at both exciting wavelengths was recorded continuously until the transient was observed, which was indicated by a deflection of the signals at 350 nm and 385 nm in opposite directions. Immediately after the transient was over, the cell was observed with Nomarski optics, which is indicated by the break in the record. The separation of chromosomes was clearly evident; they appeared as parallel rods separated by an estimated 1 μm. Poleward migration continued throughout the period of visual inspection.



cles of dye ester, which can precipitate if too much ester or not enough cells or dispersing agents are present. Use of serum albumin, Pluronic F-127 (17), and room temperature for loading (Fig. 1) sufficed to prevent this problem. We confirmed that the cytosolic dye trapped by this loading procedure was fully hydrolyzed and responsive to  $\text{Ca}^{2+}$  by treating the cells with  $1 \mu\text{M}$  of the  $\text{Ca}^{2+}$  ionophore, ionomycin, which gave 350 nm/385 nm fluorescence ratios of 18 to 20, consistent with near saturation by  $\text{Ca}^{2+}$ . Ionomycin-treated metaphase cells are usu-

ally arrested by these unphysiologically high  $[\text{Ca}^{2+}]_i$  concentrations, in accord with the results of Siskin (18).

The brevity of the observed  $[\text{Ca}^{2+}]_i$  pulse, about 20 seconds out of the 20 minutes of mitosis, explains why it would easily have been missed in previous studies (9, 10) in which  $[\text{Ca}^{2+}]_i$  was measured at only one or a few moments during mitosis. Our results do not show long-lasting localizations of high free  $[\text{Ca}^{2+}]$  at the spindle poles, so they argue against the hypothesis that such localized  $\text{Ca}^{2+}$  directly and reversibly regulates

microtubule depolymerization. Present evidence (5) indicates that microtubule depolymerization by  $\text{Ca}^{2+}$ -calmodulin requires at least  $1 \mu\text{M}$   $\text{Ca}^{2+}$ , which is higher than seen here or in previous work (8, 10). Moreover, PtK<sub>1</sub> chromosomes continue to migrate to the poles long after  $[\text{Ca}^{2+}]_i$  has declined to resting levels.

The brief  $[\text{Ca}^{2+}]_i$  transient at the metaphase-anaphase transition is more likely to act in a signaling capacity. One possible role for a short  $[\text{Ca}^{2+}]_i$  transient might be to release the connection between chromatids at the metaphase-anaphase transition. Another possible mechanism would be analogous to cytosolic factor, as described by Masui (19). Cytostatic factor activity arrests frog eggs in meiotic metaphase but is abolished by exposure to calcium. Perhaps an analogous activity exists in mitotic cells. Finally, calcium might still affect microtubules indirectly, for example, by regulating the phosphorylation state of microtubule-associated proteins (20–22). Such a cascade would allow a delocalized calcium pulse to have an effect spatially restricted by the localization of calmodulin and temporally extended by the persistence of phosphorylation states.

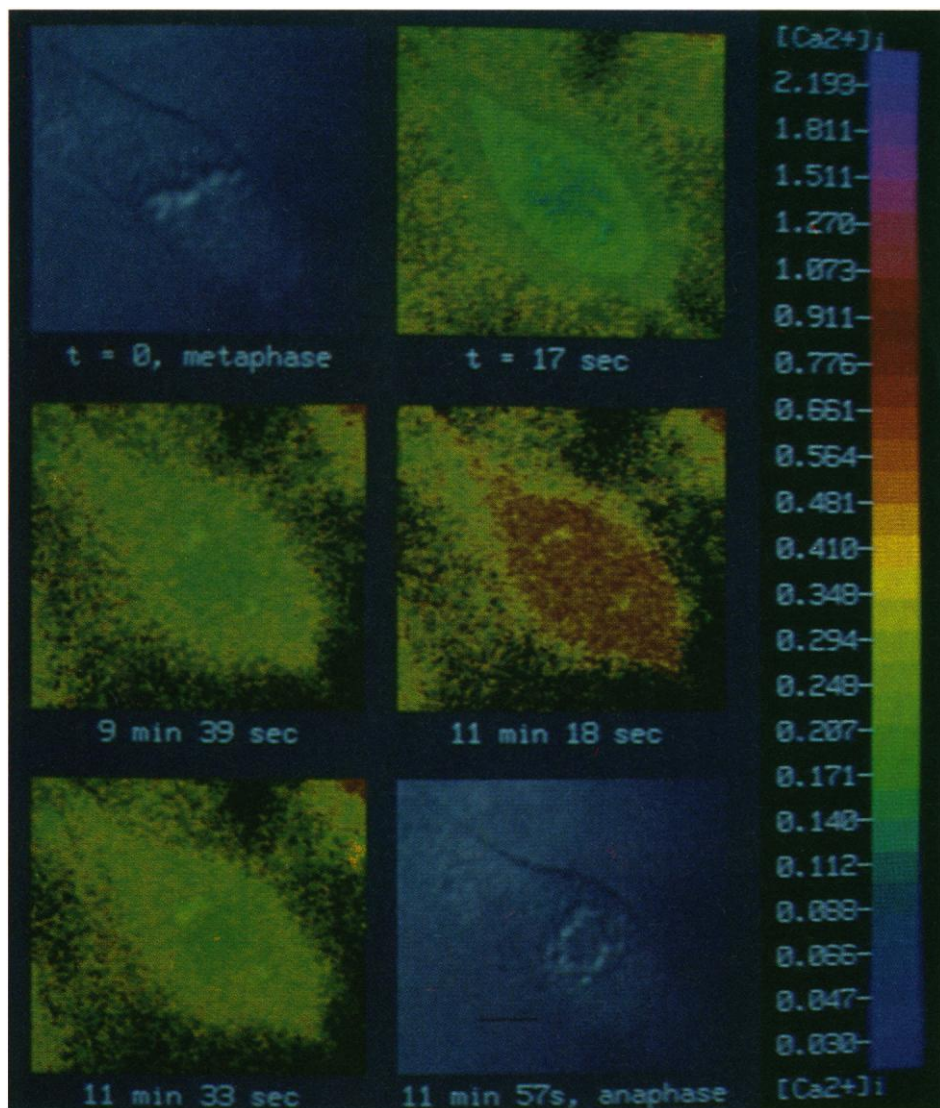


Fig. 2. A sequence of transmitted-light photographs and corresponding fluorescence ratio images shows the brief rise in  $[\text{Ca}^{2+}]_i$  throughout the cell at the onset of anaphase. Fluorescence ratios are displayed as hues that correspond to the  $[\text{Ca}^{2+}]_i$  ( $\mu\text{M}$ ) values on the right-hand color scale. Details of image acquisition, processing, and display are as described (14). A transmitted-light image ( $t = 0$ ) and corresponding fluorescence ratio image ( $t = 17$  seconds) shows the  $[\text{Ca}^{2+}]_i$  distribution at metaphase. The  $[\text{Ca}^{2+}]_i$  transient seen at  $t = 11$  minutes 18 seconds, although somewhat lower, is qualitatively similar to that shown in Fig. 1. One reason for the differences in magnitude is the 1-second accumulation time at each wavelength for the imaging experiments. Even at this relatively fast rate of data acquisition, fast transients such as observed here will be somewhat dampened. Out of 20 cells, 13 cells showed a  $[\text{Ca}^{2+}]_i$  transient and 10 of the 13 also showed concurrent chromosome separation. Of the remaining cells, six showed no transient and no separation during the period they were monitored. These cells were eventually rejected mainly due to low fluorescence signal. Finally, one cell progressed through metaphase without showing a transient that was possibly missed during transmitted-light inspection of the cell. The bar represents  $10 \mu\text{m}$ .

#### REFERENCES AND NOTES

1. P. K. Hepler and S. M. Wolniak, *Int. Rev. Cytol.* **90**, 169 (1984).
2. A. R. Means and J. R. Dedman, *Nature (London)* **285**, 73 (1980).
3. J. G. Izant, *Chromosoma* **88**, 1 (1983).
4. P. K. Hepler, *J. Cell Biol.* **100**, 1363 (1985).
5. M. Schliwa, U. Euteneuer, J. C. Bulinski, J. G. Izant, *Proc. Natl. Acad. Sci. U.S.A.* **78**, 1037 (1981).
6. G. B. Boder, D. C. Paul, D. C. Williams, *Eur. J. Cell Biol.* **31**, 399 (1983).
7. C. H. Keith, M. DiPaola, F. R. Maxfield, M. L. Shelanski, *J. Cell Biol.* **97**, 42a (1983).
8. M. Poenie, J. Alderton, R. Y. Tsien, R. A. Steinhart, *Nature (London)* **315**, 147 (1985).
9. C. H. Keith, F. R. Maxfield, M. L. Shelanski, *Proc. Natl. Acad. Sci. U.S.A.* **82**, 800 (1985).
10. C. H. Keith, R. Ratan, F. R. Maxfield, A. Bajer, M. L. Shelanski, *Nature (London)* **316**, 848 (1985).
11. G. Gryniewicz, M. Poenie, R. Y. Tsien, *J. Biol. Chem.* **260**, 3440 (1985).
12. R. Y. Tsien, T. J. Rink, M. Poenie, *Cell Calcium* **6**, 145 (1985).
13.  $[\text{Ca}^{2+}]_i$  values are calculated from fura-2 ratios  $R$  by the equation  $K(R - R_{\min})/(R_{\max} - R) = [\text{Ca}^{2+}]_i$  where  $R_{\min}$  and  $R_{\max}$  are the 350 nm/385 nm ratios obtained in zero or saturating calcium concentrations (8, 11).  $K$  is the product  $K_D(F_0/F_s)$ , where  $K_D$  is the effective dissociation constant,  $F_0$  is the 385-nm excitation efficiency in the absence of calcium and  $F_s$  is the 385-nm excitation efficiency at saturating calcium concentrations. However, the parameters  $R_{\min}$  and  $R_{\max}$  appear to be somewhat different inside cells than in conventional nonviscous calibration buffers (12). Increased viscosity enhances the fluorescence of fura-2 disproportionately at longer wavelengths so that  $R_{\min}$  and  $R_{\max}$  are shifted downward relative to values obtained under identical conditions in nonviscous solutions. This phenomenon may explain the very low  $[\text{Ca}^{2+}]_i$  reported by Keith *et al.* (9) for PtK<sub>2</sub> cells since quin-2 fluorescence excitation ratios are also severely affected by viscosity. The consensus of several different methods of correction for cytoplasmic microviscosity of PtK<sub>1</sub> cells gives corrected  $R_{\min}$  and  $R_{\max}$  values equal to 0.85 times the value obtained in nonviscous calibration solutions. We have found no evidence for a change in effective  $K_D$  with viscosity.

At basal  $[Ca^{2+}]_i$  the corrected values are 30 to 35 nM higher than what would be obtained with  $R_{min}$  and  $R_{max}$  from nonviscous calibration standards. The numerical effect of the above viscosity corrections happens to be quite similar to those used by Almers and Neher (16) but may vary with cell type and optical equipment.

14. Video images were acquired by a silicon-intensified target camera (model 66, Dage-MTI Inc., Michigan City, IN) mounted at the 35-mm camera port of an IM35 microscope that was equipped with a Nikon  $\times 40$  objective lens. The high voltage and gain of the camera were kept under manual control so that they were constant for any pair of wavelengths. The gamma correction in the camera was defeated so that camera output voltage would be directly proportional to light intensity. The TV camera output was fed both into a monitor screen and the image processor, an FD5000 from Gould Imaging and Graphics, San Jose, CA. All operations of the Gould FD5000 were controlled by a MicroPDP 11/73 (Digital Equipment Corp., Maynard, MA).

The FD5000 digitized the signal to 8-bit resolution and summed successive frames, typically 32, at each of the two excitation wavelengths. The summed wavelengths were normalized by the number of frames accumulated, and then prerecorded background images were subtracted to cancel out camera dark current and any autofluorescence due to microscope optics or in the media; these background images were acquired with the sample chamber filled with media but without cells. Cellular autofluorescence was not detectable at the excitation

light levels and camera gain settings used. Once the two images of the cells at the different wavelengths were corrected for backgrounds, their sum was calculated in one memory bank while the difference of their logarithms was deposited in another memory bank. The difference of their logarithms or log-of-ratio between corresponding picture elements contains the information as to  $[Ca^{2+}]_i$  level, but also reflects variations across the picture in the ratio between the strengths of the exciting beams. To compensate for these variations, a log-of-ratio image was prerecorded at the beginning of the experiment of a uniform thin layer of fura-2 solution in EGTA buffer trapped between two coverslips. Any nonuniformities in this log-of-ratio image of uniform dye indicated imbalances between the two excitation beams. Subtraction of this prestored log-of-ratio image largely corrected for these imbalances and normalized all ratios against the excitation ratio for the dye in EGTA buffer. Finally, the sum image and the corrected log-of-ratio image were merged into a single image containing 8 bits of information at each picture element—3 bits coded for the mean intensity of the two fluorescences and the remaining 5 bits coded for the corrected log ratio of the two fluorescences. The 3 bits of mean intensity controlled the brightness of the pseudocolor display over 8 possible values, while the 5 bits of log ratio controlled the hue over 32 shades from indigo through blue, green, yellow, orange, and red to magenta. Because the mean fluorescence intensity is coded as display brightness of each picture element, the image appears black between cells, even though the log ratio

of the two signals, fluctuating near zero, is very noisy. Dim or bright regions of the output display show where the fluorescence was weak or strong, respectively, the latter giving more reliable  $[Ca^{2+}]_i$  values. Acquisition of one complete pseudocolor image (512 horizontal  $\times$  486 vertical picture elements, each 8 bits) typically requires somewhat less than 3 seconds, of which 1.07 seconds is used for accumulating 32 frames at wavelength 1, 0.25 second for letting the image decay in the camera, 1.07 seconds for wavelength 2, and about 0.3 second to do the corrections and calculate the pseudocolor  $[Ca^{2+}]_i$  image.

15. D. A. Williams, K. E. Fogarty, R. Y. Tsien, F. S. Fay, *Nature (London)* **318**, 558 (1985).
16. W. Almers and E. Neher, *FEBS Lett.* **192**, 13 (1985).
17. L. B. Cohen *et al.*, *J. Membr. Biol.* **19**, 1 (1974).
18. J. Siskin, in *Nuclear-Cytoplasmic Interactions in the Cell Cycle*, G. L. Whitson, Ed. (Academic Press, New York, 1980), pp. 271–292.
19. Y. Masui, M. J. Lohka, E. K. Shibuya, *Symp. Soc. Exp. Biol.* **38**, 45 (1984).
20. H. Schulman, *J. Cell Biol.* **99**, 11 (1984).
21. ———, J. Kuret, A. B. Jefferson, P. S. Nose, K. H. Spitzer, *Biochemistry* **24**, 5320 (1985).
22. D. Job, C. T. Rauch, E. H. Fischer, R. L. Margolis, *Proc. Natl. Acad. Sci. U.S.A.* **80**, 3894 (1983).
23. Supported by grants from NIH (GM31004 and EY04372) and the Searle Scholars Program to R.Y.T. and NSF grant PCM 84-02089 to R.A.S.

14 February 1986; accepted 6 June 1986

## Upstream Operators Enhance Repression of the *lac* Promoter

MICHAEL C. MOSSING\* AND M. THOMAS RECORD, JR.

To study regulation of transcription by distant elements, a wild-type *lac* operator was inserted upstream of a promoter-constitutive operator control region. The upstream operator is shown to aid in repression of transcription from the mutant control region. The effectiveness of the upstream operator as a function of its distance from the mutant control region parallels the length dependence observed for DNA cyclization. A quantitative model is proposed for action-at-a-distance of DNA control sites in which protein-protein and protein-DNA interactions are mediated by DNA looping. In this model, the effective concentrations of interacting proteins that are tethered by DNA are determined by the length of the intervening DNA and by its inherent bending and torsional stiffness. This model makes a number of predictions for both eukaryotic and prokaryotic control sequences located far from their sites of action.

THE *lac* OPERON HAS SERVED AS A paradigm for the molecular mechanism of gene regulation (1). Recently, however, eukaryotic systems have been described that appear not to conform to this classic model of direct interaction of activator and repressor proteins with RNA polymerase at the transcription start point (2). Specifically, regulatory sites have been identified that function irrespective of orientation and at large and variable distances from the site of initiation of RNA synthesis. In the *lac* operon, binding sites for *lac* repressor far removed from the classical operator site at the start of transcription have been identified (3, 4). Although in the wild-type operon these sites have had no proven role, we have proposed that they may aid in repres-

sion of a constitutive mutant ( $O^c$ ) operator (5).

In this study we demonstrate that operators inserted at various distances upstream of a *lac* promoter- $O^c$  operator pair enhance repression in vivo. Furthermore, this effect is length-dependent. The similarities between the distance dependence we observe for cooperative repression and that observed for DNA cyclization reactions (6) suggest a general mechanism for the regulatory action of distant DNA sites. Qualitative models involving DNA bending and looping have been proposed to account for the interaction of proteins bound to distant DNA sites (2, 7–10). For the arabinose operon of *Escherichia coli*, data obtained both in vivo and in vitro have been interpreted in terms of the

looping model (7). Consideration of the three-dimensional distribution of DNA sites that are distant along the primary sequence of the DNA puts these models in a new light. Instead of merely impeding complex formation through the requirement for bending or distortion, the intervening DNA acts as a tether which can increase the concentration of one site (or its associated protein) in the vicinity of a second site, thus driving the interaction in a quantitatively predictable manner.

A *lac* promoter-constitutive operator control region has been fused to the galactokinase gene of pKO4 (11) to make the plasmid pKO<sup>c</sup> (Fig. 1). The  $O^c$  mutation has thus been removed from the context of the *lac* operon and the pseudo operators that have been identified at the end of the *I* gene (3) and  $\sim 370$  bp into the *Z* gene (4). To demonstrate the effect of distant operators directly, we constructed a series of plasmids with a wild-type *lac* operator placed at various positions upstream from the mutant operator in pKO<sup>c</sup>. This configuration maximizes our chances of observing an effect, since an  $O^c$  operator in the control site both increases the basal level of expression and ensures that the auxiliary ( $O^+$ ) site will be the preferred binding site for repressor. Table 1 lists the results of galactokinase and  $\beta$ -galactosidase activity measurements on cells

Department of Chemistry and Biochemistry, University of Wisconsin-Madison, Madison, WI 53706.

\*Present address: Department of Biology, Massachusetts Institute of Technology, Cambridge, MA 02139.